Proceedings of the IASS 2024 Symposium
Redefining the Art of Structural Design
August 26-30, 2024, Zurich Switzerland
Philippe Block, Giulia Boller, Catherine DeWolf,
Jacqueline Pauli, Walter Kaufmann (eds.)

Timber groin vault floor system for low embodied carbon buildings

Shane HOSSELL*, Will HAWKINS, Antony DARBY, Tim IBELL

* University of Bath
Calverton Down, Bath, BA2 7AY
smh95@bath.ac.uk

Abstract

This study explores whether parabolic groin vaults constructed from cross-laminated timber (CLT) can significantly reduce the embodied carbon of structures, which currently contribute approximately 10% of global greenhouse gas emissions. The groin vault system is constructed by alternately gluing parabolically curved longitudinal lamellas with straight transverse lamellas. Steel ties counter the horizontal thrust forces produced by the vault and ribs provide a level surface. The study minimises the embodied carbon for spans ranging from 6-14m through parametric modelling, optimisation using genetic algorithms, and structural analysis with shell elements. Key optimisation parameters include the vault's rise, the thickness and number of lamellas, and the diameter of the steel ties. The model accounts for the anisotropic stiffness and strength of cross laminated timber, as well as the fabrication stresses and vibration performance. The embodied carbon of the sawn timber, material wastage due to planing, adhesives, and the steel ties are considered. Compared to CLT flat slabs with equivalent structural performance, the study reveals potential embodied carbon savings (54%-64%) for floor spans ranging from 6m to 14m. These results show that considerable embodied carbon savings can be achieved by harnessing the strength and renewable benefits of timber in conjunction with the geometric stiffness advantages of vaults.

Keywords: Timber vaults, Cross-laminated timber, Timber floors, Embodied carbon, Structural optimisation, Anisotropic timber behaviour, Vibration performance, Sustainable construction, Parametric modeling

1. Introduction

Amidst escalating global environmental challenges, a paradigm shift in the choice of materials and structural form is imperative to ensuring a sustainable construction industry. Modern construction methods, which are particularly reliant on steel and concrete, currently account for more than 10% of global energy-related emissions [1]. With the expected doubling of building floor area by 2060, it is imperative to shift towards more sustainable construction methods to align with the Paris Agreement's 1.5°C global warming limit [2]. This paper explores the potential of parabolic cross-laminated timber (CLT) floors as a method to reduce the overall embodied carbon of structures by utilising the renewable and strength properties of timber in combination with the geometric stiffness of vaults.

The anisotropic behaviour of timber in conjunction with the CLT lamellas being placed perpendicular to each other in each sequential layer adds additional complexity to the analysis [4]. Timber and CLT's relatively low stiffness, compared to concrete and steel, often restricts its use in long-span applications due to deflection and vibration limits, which require deep members resulting in the majority of the material being under-utilised when used as bending elements [5].

Timber vaults, on the other hand, share similar compression and bending characteristics with trees and benefit from increased structural stiffness due to their geometry, which has enabled large free spans [6]. Although the manufacture of curved timber structures adds complexity, this can be achieved through steam bending, lamination, and kerfing, enabling a departure from traditional straight timber construction to more innovative lightweight vaulted structures [7], [8]. Previous studies on vaulted concrete floors have demonstrated potential carbon savings relative to bending structures [9] and therefore it is expected that timber vaulted floors will offer comparable or even greater savings of embodied carbon.

2. Problem statement and methodology

The study aims to assess the feasibility of using parabolic cross-laminated timber groin vaults as a low embodied carbon alternative to conventional cross-laminated timber floors by exploring spans between 6m and 14m. Figure 1 presents the proposed floor design, combining curved longitudinal lamellas and straight transverse lamellas to make up the four barrel vault segments of the groin vault. Timber ribs create a level surface. Granular infill material, consisting of either dry aggregates or sand sourced from land won or recycled materials, is proposed to improve the vibration performance by adding mass and damping. This material can be evenly distributed to create a level surface or selectively distributed in targeted areas to improve the dynamic performance without requiring a substantial increase in vault strength. Additionally, the voids above and below the vault can accommodate building services, that would otherwise be accommodated using suspended ceilings in conventional flooring systems.

The initial assessment, discussed in this paper, concentrated on optimising the groin vault solely for strength and deflection serviceability, without considering the use of granular infill material. Utilising the optimal solution, vibration response was determined, and potential mitigation strategies are discussed if required.

This study examines office floor loadings, incorporating a live load of 3.5 kN/m^2 (2.5 kN/m^2 office loading and 1 kN/m^2 for movable partitions), superimposed dead load of 1 kN/m^2, and material densities shown in Table 1 [10]. Instantaneous and long-term serviceability limit state (SLS) deflections are set to Span/300 and Span/250, respectively, accounting for creep and moisture under service class 1. The analysis includes three live loading scenarios: full, half, and quarter loading.

Parametric model was developed in Python utilising a linear elastic model in PyMAPDL [11], using Shell 181 elements for the groin vault and Beam 188 for the ties to include shear deformation [12]. The stiffness of the ribs was not considered in the analysis. The genetic algorithm PyGAD [13] module was selected as it can easily handle both discrete and continuous variables.

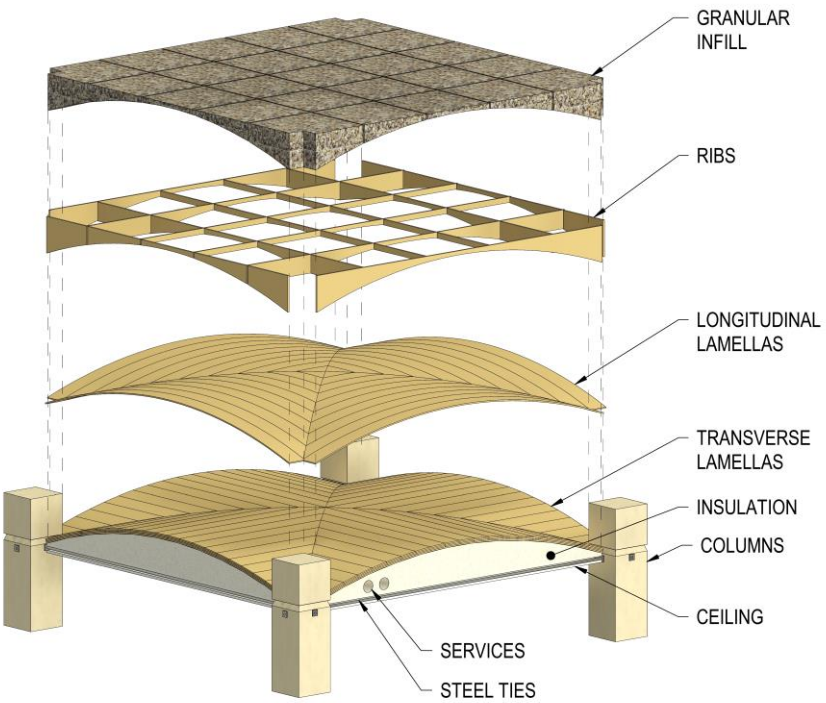

Figure 1 Proposed cross-laminated groin vault timber floor: Illustrating the curved longitudinal lamellas and straight transverse lamellas in alternating layers, with the addition of ribs to create a level surface and ties to restrain the horizontal thrust forces.

The groin vault was optimised in terms of rise (h), longitudinal lamella thickness(t_L), transverse lamella thickness (t_t), number of lamellas, and steel tie diameter ($\varnothing_{tie}$). Only odd number of lamellas are used in the analysis for section symmetry.

The Van der Put anisotropic strength failure model [14] is used to address the biaxial stresses in the C24 [15] cross laminated groin vault subjected to combined axial, bending and transverse shear loading. The equivalent stiffness method, outlined in Eriksson and Karlsson [16] and The CLT Handbook [17], was used to determine the stiffness of the vault in longitudinal and transverse directions. To avoid overstressing the longitudinal lamellas, shown in Figure 1, during fabrication, the lamella thickness decreases with increasing vault rise and curvature. The stress checks factored in the fabrication stresses considering 20% relaxation after 2 weeks [18]. Additionally, discussions with glulam manufacturers indicate that approximately 5mm is typically planed off the top and bottom of the lamellas, and 10mm off the sides to ensure a smooth surface for gluing, and this has been included in the optimisation process.

The floor's vibration serviceability is evaluated by calculating the response factor across the vault, following the revised Eurocode 5 criteria [19], with coinciding excitation and response points. Using the forcing function from SCI P354 [20] and modal analysis with Newmark's method [21], the floor's velocity and acceleration responses are determined, assuming a 5% damping ratio. Performance is assessed through the root mean square acceleration for resonant floors ($f_n \leq 8$Hz) or velocity (υ_{rms}) for impulsive floors ($f_n > 8$Hz). The calculated response factor is compared to the revised Eurocode 5 [19], with a response factor below R = 8 deemed satisfactory for offices [22].

2.1. Embodied carbon model

The performance of the groin vault is evaluated using an objective function in terms of embodied carbon, limited to cradle-to-gate emissions (A1-A3) [3]. Table 1 outlines the embodied carbon factors, which includes emissions from sawn timber (felling, transport, kiln drying), planing wastage, steel ties, and granular infill material. Timber and steel embodied carbon values were obtained from environmental product declarations [23] [24]. Melamine-urea formaldehyde (MUF) resin is selected for its cost effectiveness and reliability [25], [26].

Table 1 Embodied carbon factors and densities for each material within the proposed system

Material	**Sawn timber (C24)**	**Adhesive (MUF)**	**Steel**
Density (kg/m3)	460	-	7850
Embodied carbon ($kgCO_2e/kg$)	0.074	1.775	0.68

To incorporate the Ultimate Limit State (ULS) and SLS design criteria within the genetic algorithm, a penalty term is added to the objective function (Equation 1). This term penalises solutions exceeding ULS and SLS utilisation values of 1, applying larger penalties for higher exceedance. The total objective function (EC_{A1-A3}) is calculated by summing the embodied carbon factors (ECF_i) multiplied by either the mass, volume, or area (Q_i) of each material or process, plus any penalties (P) for design options that exceed the ULS or SLS deflection constraints based on the utilisation factor (U_i).

$$EC_{A1-A3} = \sum_{i=1}^{n}(ECF_i \times Q_i) + \sum_{i=1}^{m} P\left(1 - \frac{1}{U_i}\right) \text{ If } U_i < 1 \text{ then } U_i = 1 \quad (1)$$

3. Results and discussion

3.1. Strength optimisation

For all the analysed spans, the half load distribution governed the strength utilisation, as shown in Figure 2, for the 8m span, due to the introduction of significant bending stresses. Figure 2 shows that the maximum utilisation primarily occurs at the supports and along the creases between segments. Stresses within 200mm from the supporting edges were excluded due to mesh-dependant peak values and resultant stress concentrations, particularly around the re-entrant corners. To address these regions, manual strength checks were undertaken by resolving the reactions into the axial, shear, and twisting loads and calculating the resultant stresses. To prevent the supports from governing the overall vault thickness, the inclusion of steel flinch plates or localised thickening of the vault around the supports can be considered. Additionally, the below figure shows that a large portion of the vault shows lower utilisation, indicating potential for further optimisation. For instance, incorporating beams along the groins could reduce the stresses and, hence, overall thickness of the vault.

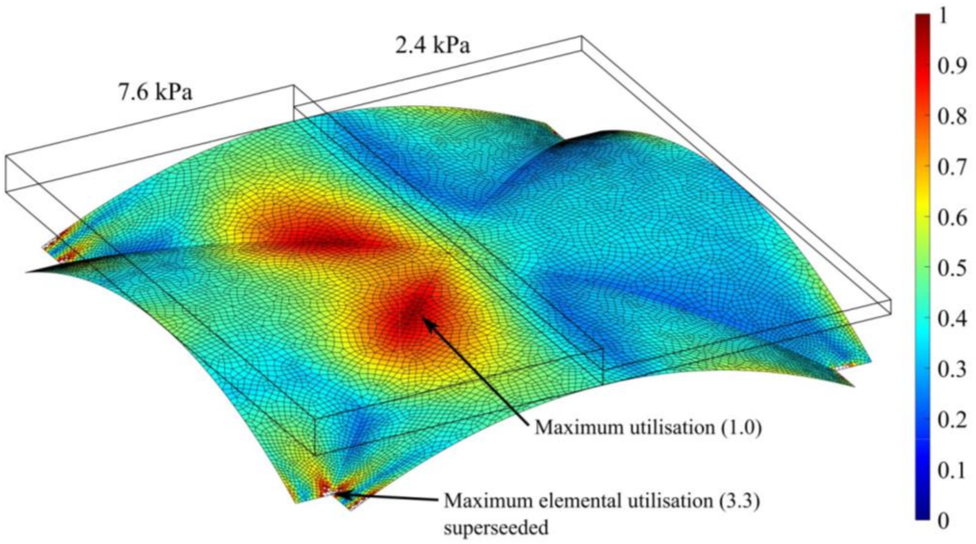

Figure 2 Maximum strength utilisation within the section per element across the shell surface

3.2. Vibration results

Utilising the strength and deflection limit optimal solution, vibration performance assessment was undertaken on the vault to determine the peak response factor and whether additional strategies would need to be considered in order to achieve the required performance. Utilising the results from the 8m floor, modal analysis is used to determine the natural frequencies, modal masses, and mode shapes without granular infill material or rib stiffness, resulting in a fundamental frequency of 10.5Hz and first mode mass participation of 3130 kg, indicative of impulsive behaviour. Figure 3 illustrates the response factor across the vault floor with 5% damping, when the excitation and response points coincide. The centre of the vault has the highest response factor, which aligns with the fundamental mode shape. The floor's maximum response slightly exceeds 8, going beyond the accepted limit for office floors [19].

To reduce the response factor, granular infill material can be strategically added around the vault's centre, aligning with the primary mode shape, increasing mass and damping. However, as granular infill doesn't add stiffness, this extra mass will lower the floor's natural frequency, risking resonance behaviour and a higher response factor. Therefore, it is desirable to prevent the fundamental frequencies from aligning with the first four pacing frequency harmonics, whilst maximising the infill's damping and acoustic benefits. Additionally, the infill mass will result in a larger dead load requiring a thicker vault and larger thrust forces, which concomitantly will require a larger tie diameter. However, the analysis conservatively ignores the rib stiffness, which is expected to improve the structure's vibration response.

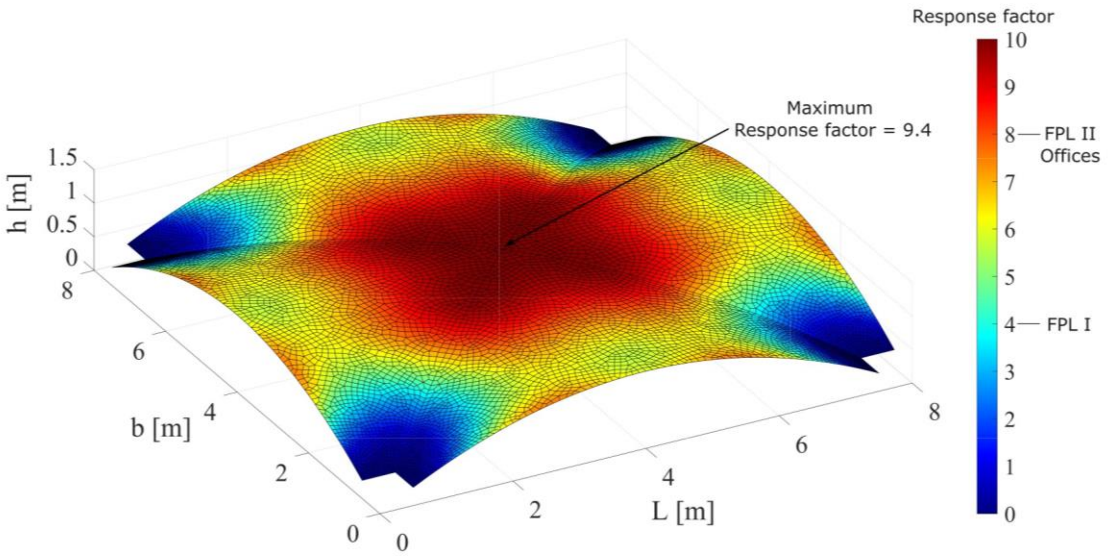

Figure 3 Calculation of the response factor across the floor area, with the excitation and response locations coinciding at the same location. The figure also shows the Floor perfomance level (FPL), as determined by the criteria in the revised Eurocode 5 [19] with a FPL II being satisfactory for office floors.

3.3. Embodied carbon savings

Figure 4 shows the optimal solutions for the proposed groin vault system and an equivalent optimised CLT flat slab solution, and shows that significant embodied carbon savings can be achieved by adding curvature and incorporating a steel tie to restrain the thrust forces. The embodied carbon savings range from 54% to 63%, becoming more pronounced at longer spans. The design of the CLT flat slabs is primarily governed by long-term deflection limits, due to the relatively low bending stiffness of timber, which becomes more significant at longer spans. The geometry of the groin vaults effectively shifts the primary design from deflection serviceability to strength, allowing for thinner sections, less adhesive, and significantly lower embodied carbon, with the benefits becoming more pronounced at longer spans.

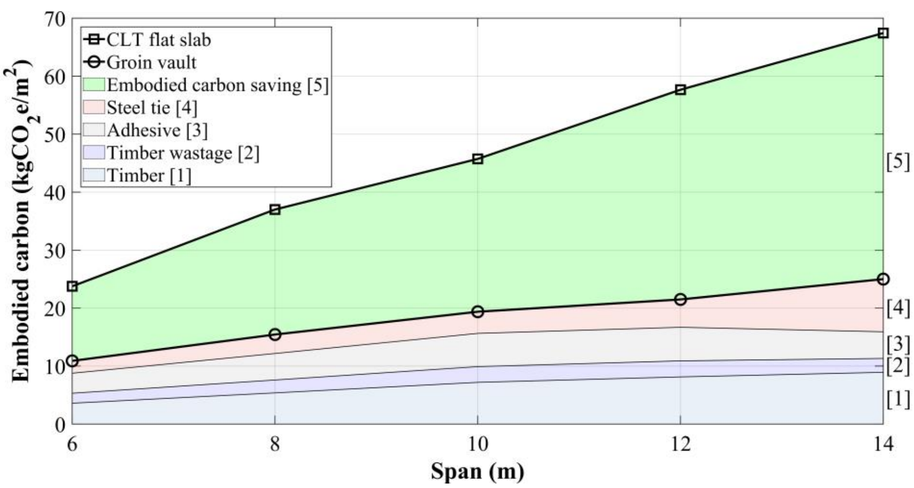

Figure 4 Variation of embodied carbon with span for the proposed system and an equivalent CLT floor. The embodied carbon breakdown of each component's contribution that makes up the groin vault is also shown.

However, the designs where optimised with a single timber and steel embodied carbon value and therefore the sensitivity of the design to varying steel and timber embodied carbon values still needs to be investigated. It is anticipated that as the ratio of the steel's embodied carbon factor to that of timber increases, the feasibility of the proposed solution will only occur with a further increase in span. At higher steel embodied carbon values, the vault design must compensate by increasing the rise to reduce horizontal thrust forces, and the subsequent reduction in the steel's embodied carbon. However, with increased rise, fabrication stresses necessitate thinner lamellas, leading to additional material wastage due to planing. Consequently, the design may revert to a CLT flat slab solution. The use of steel with a higher recycled content and produced using electric arc furnaces (EAF) powered by renewable energy will enhance the feasibility of floor system.

4. Conclusions and future research

This study demonstrates that using a parabolic cross-laminated timber optimised (CLT) structures can achieve long span floors with significant reduction in embodied carbon of over 50%. By integrating optimisation techniques, such as genetic algorithms, in the design process, parabolic cross laminated timber (CLT) shell structures have been optimised for minimal embodied carbon that considers both the materials and fabrication process.

The groin vault system changes the primary design limiting criteria from deflection to strength, however, vibration serviceability limit states need to be integrated into future optimisations as the design could be either strength governed or vibration serviceability governed. The embodied carbon savings of the vaults is span dependent with the savings becoming more pronounced at longer spans. Also, the ratio of embodied carbon between steel and timber influences the feasibility of the solution as higher steel to timber embodied carbon ratios results in the solution favouring a flat slab solution over greater span lengths.

Future optimisations will consider the dynamic response at the centre of the groin vault to determine the impact it has on the optimal solution. The practical aspects of fabricating groin vaults, including automated fabrication, connections, and multi-objective optimisation including the impact of labour costs and vault height on the solution will also be investigated. The potential benefits of adding rib stiffness and granular infill material into the model will also be investigated. Experimental work will be undertaken on a scaled groin vault model to validate the model and determine the vibration characteristics of the groin vault. Further studies will be undertaken comparing the embodied carbon savings with other optimal and lightweight timber solutions such as timber I-beams, corrugated timber floor systems, and other proprietary timber joist systems, to determine the embodied carbon savings, which is postulated to be more beneficial at longer spans.

Acknowledgements

We gratefully acknowledge the support of EPSRC DTP studentship [Number: EP/T518013/1], UK FIRES [EP/S019111/1]

References

[1] United Nations Environment Programme, 2020 Global Status Report for Buildings and Construction: Towards a Zero-emission, Efficient and Resilient Buildings and Construction Sector. Nairobi: United Nations, 2020. Accessed: Jan. 16, 2023. [Online]. Available: https://globalabc.org/sites/default/files/inline-files/2020%20Buildings%20GSR_FULL%20REPORT.pdf

[2] IEA, 'Net Zero by 2050', IEA: Paris, 2021, [Online]. Available: https://www.iea.org/reports/net-zero-by-2050, License: CC BY 4.0

[3] O. Gibbons and J. Orr J., How to calculate embodied carbon, Second. London, United Kingdom: The Institution of Structural Engineers, 2022. [Online]. Available: https://www.istructe.org/resources/guidance/how-to-calculate-embodied-carbon/

[4] A. A. Chiniforush, A. Ataei, H. R. Valipour, T. D. Ngo, and S. Malek, 'Dimensional stability and moisture-induced strains in spruce cross-laminated timber (CLT) under sorption/desorption isotherms', Construction and Building Materials, vol. 356, p. 129252, Nov. 2022, doi: 10.1016/j.conbuildmat.2022.129252.

[5] J. Zhang, H. Shen, R. Qiu, Q. Xu, and S. Gao, 'Short-term flexural behavior of prestressed glulam beams reinforced with curved tendons', Journal of Structural Engineering, vol. 146, no. 6, p. 04020086, 2020.

[6] R. Crocetti, ‘Large-span timber structures’, in Proceedings of the World Congress on Civil, Structural, and Environmental Engineering, 2016, pp. 1–23.
[7] L. Aldinger, S. Bechert, D. Wood, J. Knippers, and A. Menges, ‘Design and Structural Modelling of Surface-Active Timber Structures Made from Curved CLT - Urbach Tower, Remstal Gartenschau 2019’, in Impact: Design With All Senses, C. Gengnagel, O. Baverel, J. Burry, M. Ramsgaard Thomsen, and S. Weinzierl, Eds., Cham: Springer International Publishing, 2020, pp. 419–432. doi: 10.1007/978-3-030-29829-6_33.
[8] C. Robeller, S. S. Nabaei, and Y. Weinand, ‘Design and Fabrication of Robot-Manufactured Joints for a Curved-Folded Thin-Shell Structure Made from CLT’, in Robotic Fabrication in Architecture, Art and Design 2014, W. McGee and M. Ponce de Leon, Eds., Cham: Springer International Publishing, 2014, pp. 67–81. doi: 10.1007/978-3-319-04663-1_5.
[9] W. Hawkins, J. Orr, P. Shepherd, and T. Ibell, ‘Design, Construction and Testing of a Low Carbon Thin-Shell Concrete Flooring System’, Structures, vol. 18, pp. 60–71, Apr. 2019, doi: 10.1016/j.istruc.2018.10.006.
[10] EN 1991-1-1, ‘Eurocode 1: Actions on Structures. Part 1-1: General Actions — Densities, Self-weight, Imposed Loads for Buildings’. London: British Standards Institution, 2002.
[11] PyAnsys, ‘PyMAPDL: Python Interface for ANSYS Mechanical APDL’. 2024. [Online]. Available: https://mapdl.docs.pyansys.com/version/stable/index.html
[12] A. C. Ugural and S. K. Fenster, Advanced mechanics of materials and applied elasticity. Pearson Education, 2011.
[13] A. F. Gad, ‘PyGAD - Python Genetic Algorithm’. 2024. [Online]. Available: https://pygad.readthedocs.io/en/latest/index.html
[14] T. Van der Put, ‘The tensorpolynomial failure criterion for wood’, Delft Wood Science Foundation, Delft, 2005.
[15] BS EN 338, ‘BS EN 338 Structural timber. Strength classes’. London: British Standards Institution, 2016.
[16] R. Eriksson and M. Karlsson, Effect of birch in CLT elements: An investigation of how introducing birch effects the strength properties of CLT elements. 2020.
[17] Swedish Forest Industries Federation, The CLT Handbook, 1st UK ed. Stockholm, Sweden: Swedish Forest Industries Federation, 2019.
[18] A. J. Lara-Bocanegra, A. Majano-Majano, F. Arriaga, and M. Guaita, ‘Long-term bending stress relaxation in timber laths for the structural design of lattice shells’, Construction and Building Materials, vol. 193, pp. 565–575, Dec. 2018, doi: 10.1016/j.conbuildmat.2018.10.224.
[19] W. Schirén and T. Swahn, ‘Vibrations in residential timber floors: A comparison between the current and the revised Eurocode 5’, 2019.
[20] A. L. Smith, S. J. Hicks, and P. J. Devine, ‘Design of Floors for Vibration: A New Approach’, p. 128, 2009.
[21] A. K. Chopra, Dynamics of structures: theory and applications to earthquake engineering, 4th ed. Upper Saddle River, N.J: Prentice Hall, 2012.
[22] M. Willford and P. Young, ‘A Design Guide for Footfall Induced Vibration of Structures: A tool for designers to engineer the footfall vibration characteristics of buildings or bridges’. The Concrete Society: Surrey, 2006.
[23] Stora Enso, ‘Environmental Product Declaration in accordance with ISO 14025 and EN 15804 for: Classic Sawn. EPD International AB. EPD registration number: S-P-02150.’ 2020.
[24] M. Fishwick and K. Livesey, ‘Environmental product declaration (EPD) report of fabricated steel products produced in the UK by Eco-Reinforcement members’. BRC Ltd, 2019.
[25] M. Dunky, ‘Urea–formaldehyde (UF) adhesive resins for wood’, International Journal of Adhesion and Adhesives, vol. 18, no. 2, pp. 95–107, Mar. 1998, doi: 10.1016/S0143-7496(97)00054-7.
[26] S. Park, B. Jeong, and B.-D. Park, ‘A Comparison of Adhesion Behavior of Urea-Formaldehyde Resins with Melamine-Urea-Formaldehyde Resins in Bonding Wood’, Forests, vol. 12, no. 8, p. 1037, Aug. 2021, doi: 10.3390/f12081037.